Effects of the screened exchange interaction on the tunneling and Landau gaps in double quantum wells

Danhong Huang and M. O. Manasreh
Phillips Laboratory (PL/VTRP), 3550 Aberdeen Avenue SE, Building 426, Kirtland Air Force Base, New Mexico 87117
(Received 2 January 1996)

A self-consistent screened Hartree-Fock calculation, combined with the Landau quantization of in-plane electron motion, is performed to find the eigenstates and eigenenergies of electrons in double quantum wells. This theory is applicable to both the low and strong magnetic-field cases. The screened exchange interaction is calculated by using a generalized Thomas-Fermi screening model. The approximately linear increase of the tunneling gap at low magnetic fields ($B<9$ T) and the switching of the ground state between the tunneling-split first Landau levels are seen and explained as a result of the increase of screening effects on the exchange interaction when both tunneling-split first Landau levels are filled. [S0163-1829(96)00623-6]

There have long been both theoretical and experimental interests in double-quantum-well structures in the presence of an external magnetic field. The destruction of integer quantum Hall states with odd filling factors in double-quantum-well structures and in a single wide quantum well was observed recently.[1–3] Several theoretical explanations[4–6] were given for these observations. Also, the collapse of the fractional quantum Hall states in the single wide quantum well[7] and half integer fractional quantum Hall state in the double-quantum-well structure[8,9] was reported. The theoretical explanations to these experimental findings were proposed[10–12] for both single wide quantum-well and double-quantum-well structures. Some theoretical calculations on the magnetoroton excitation spectrum[13–15] and the suppression of the spin-density excitation[16,17] were shown. More recently, the effect of an in-plane magnetic field on the electron tunneling was studied both experimentally[18–22] and theoretically.[23,24]

The electron tunneling behavior in the presence of a perpendicular magnetic field was also found very interesting and nontrivial,[25,26] where instead of a $\sqrt{B}$ dependence an approximately linear B dependence of the tunneling gap from the dc measurement was observed. This behavior was first explained by Yang and MacDonald as a result of the ''Coulomb gap''[27] in the density of states when the filling factor is less than unity. Unfortunately, this explanation only produced a $\sqrt{B}$ dependence on the tunneling gap, which is not supported by a recent experiment.[26] Besides, the screening effects on the exchange interaction is neglected in their calculation.[27] The magnetoplasmon excitation in the double-quantum-well structure was also calculated.[28] However, the effect of the Landau quantization in the presence of a magnetic field was not included in the self-consistent Hartree calculation of the eigenstates and eigenenergies in the z direction. This limits the application of their theory most to the very week magnetic-field case.

In this paper, we have performed a self-consistent screened Hartree-Fock calculation combined with the Landau quantization of the in-plane electron motion to find the eigenstates and eigenenergies of electrons in a double-quantum-well structure. This theory is expected to be applicable to both low ($B<9$ T) and strong magnetic-field ($B>9$ T) cases. In our model, the screened exchange interaction is calculated using a generalized Thomas-Fermi screening model. From our numerical computation, we find the approximately linear increase of the tunneling gap at low magnetic fields ($B<9$ T) and the switching of the ground state between the tunneling-split Landau levels, which are explained as a result of the increase of screening effects on the exchange interaction when both the tunneling-split first Landau levels are filled. In our calculation, we concentrate on the strong-coupling region with thin barrier, which is out of the Coulomb gap region with a thick barrier. The predicted switching of the ground state below 9 T in this paper is different and, to our knowledge, the first reported in this system that can be observed in the cyclotron resonance experiment as an anticrossing of two resonance peaks.

The model we consider is a doped symmetric double-quantum-well (DQW) structure that contains two wells separated by a middle barrier. An external magnetic field is applied perpendicular to the planes of quantum wells. In the self-consistent screened Hartree-Fock approximation, the vertical electron motion in the z direction perpendicular to the DQW is described by the Schrödinger equation containing both the DQW potential $V_{\mathrm{DQW}}(z)$ and the self-consistent Hartree potentials $V_H(z)$,[28]

$$\left[-\frac{\hbar^2}{2}\frac{d}{dz}\left(\frac{1}{m^*(z)}\frac{d}{dz}\right)+V_{\mathrm{DQW}}(z)+V_H(z)\right]\phi_j(z)=E_j\phi_j(z), \tag{1}$$

where $j=1, 2, \ldots$ is the subband index and $m^*(z)$ is the position-dependent effective mass of electrons that varies from well to barrier materials. Meanwhile, the in-plane electron motion in each subband in the DQW is Landau quantized in the presence of a magnetic field **B** perpendicular to the DQW. In the Landau gauge, we can assign a plane wave for the electron motion in the y direction and the electron motion in the x direction is determined from another Schrödinger equation[11]

$$\left[-\frac{\hbar^2}{2m_j^*}\frac{d^2}{dx^2}+\frac{1}{2}m_j^*\omega_{cj}^2(x-X_0)^2\right]\xi_{nk_y}(x)$$
$$=\left(n-\frac{1}{2}\right)\hbar\omega_{cj}\xi_{nk_y}(x), \tag{2}$$

where $n=1, 2, \ldots$ is the Landau quantum number, m_j^* is the electron effective mass in the jth subband, which will be given below, $\omega_{cj}=eB/m_j^*$ is the cyclotron frequency in the jth subband, $X_0=-k_y l_H^2$ is the orbital guiding center in the plane, k_y is the electron wave number in the y direction, and $l_H=\sqrt{\hbar/eB}$ is the magnetic length. In Eq. (1), the shape of a symmetric DQW potential is chosen as

$$V_{\mathrm{DQW}}(z)=\begin{cases}0, & -d_W-d_B/2<z<-d_B/2 \text{ or } d_B/2<z<d_B/2+d_W\\ V_0 & \text{otherwise,}\end{cases} \tag{3}$$

where d_W is the individual well width, d_B is the middle-barrier width, and V_0 is the middle-barrier height. The Hartree potential can be directly calculated from the Poisson equation[28]

$$\frac{d}{dz}\left[\epsilon_b(z)\frac{d}{dz}V_H(z)\right]=\frac{e^2}{\epsilon_0}[n(z)-N_{im}(z)]. \tag{4}$$

In Eq. (4), $\epsilon_b(z)$ is the dielectric constant of the well or barrier bulk materials, which varies with z. $n(z)$ is the electron-density function

$$n(z)=\frac{1}{\pi l_H^2}\sum_{n,j}\left\{\frac{1}{\exp\{[E_j+(n-\frac{1}{2})\hbar\omega_{cj}-\mu_c]/k_BT\}+1}\right\}\times|\phi_j(z)|^2, \tag{5}$$

where T is the electron temperature and μ_c is the chemical potential at finite T. $N_{im}(z)$ is the donor doping density profile

$$N_{im}(z)=N_{im}^{3\mathrm{D}}(z)+\sum_i N_{im}^{2\mathrm{D}}(i)\,\delta(z-z_i), \tag{6}$$

which includes both the selective doping and δ-doping contributions, where $N_{im}^{2\mathrm{D}}(i)$ is the sheet density for δ doping in the ith layer at $z=z_i$. Because the electron effective masses in the well and barrier materials are different and by using the first-order perturbation theory, we find the ''average'' effective mass, used in Eq. (1), for the electrons in the jth subband to be[28]

$$\frac{1}{m_j^*}=\frac{P_j}{m_W}+\frac{1-P_j}{m_B}, \tag{7}$$

which depends on the subband index. Here m_W and m_B are the electron effective masses in the well and barrier materials, respectively. In Eq. (7), the electron quantum-well dwelling probability is calculated as

$$P_j=\int_{-d_B/2-d_W}^{-d_B/2}dz|\phi_j(z)|^2+\int_{d_B/2}^{d_B/2+d_W}dz|\phi_j(z)|^2. \tag{8}$$

The charge neutrality condition for the completely ionized donors leads us to

$$\int_{-\infty}^{+\infty}dz\ n(z)=n_{2\mathrm{D}}=\int_{-\infty}^{+\infty}dz\ N_{im}^{3\mathrm{D}}(z)+\sum_i N_{im}^{2\mathrm{D}}(i), \tag{9}$$

where $n_{2\mathrm{D}}$ is the areal electron density. Equation (9) can be used to determine μ_c in a self-consistent way. The total electron energy including both the in-plane and vertical electron motions can be written as

$$E_{nj}=(n-\tfrac{1}{2})\hbar\omega_{cj}+E_j+V_{nj}^F, \tag{10}$$

where V_{nj}^F is the exchange energy and will be given below. From the self-consistent equations (1)–(9), we are able to calculate the eigenstate $\phi_j(z)$ and total eigenenergy E_{nj} in each step. Consequently, the eigenstate in each step is found to be

$$\psi_{njk_y}(\mathbf{r})=\frac{\exp(ik_y y)}{\sqrt{L_y}}\sqrt{\frac{1}{\pi^{1/2}2^{n-1}n!\,l_H}}\times\exp\left[\frac{(x-X_0)^2}{2l_H^2}\right]H_{n-1}\left(\frac{x-X_0}{l_H}\right)\phi_j(z), \tag{11}$$

where $H_n(x)$ is the nth-order Hermite polynomial and L_y is the size of the sample in the y direction.[11]

Based on the calculated self-consistent wave function $\psi_{njk_y}(\mathbf{r})$ and subband edge E_{nj} in each step, we can compute the screened exchange energy that is needed to finish the self-consistent Hartree-Fock calculation. A straightforward calculation brings us to the result[29]

$$V_{nj}^F=-\frac{1}{2\pi}\sum_{n',j'}\int_0^{+\infty}dq_{xy}q_{xy}\times\left\{\frac{1}{\exp[(E_{n'j'}-\mu_c)/k_BT]+1}\right\}\times|\mathcal{A}_{n'n}(q_{xy})|^2V_{jj'}^F(q_{xy}), \tag{12}$$

where $q_{xy}=\sqrt{q_x^2+q_y^2}$ is the module of a two-dimensional wave vector $\mathbf{q}_{xy}=(q_x,q_y)$ and the form factor due to Landau quantization is

$$|\mathcal{A}_{n'n}(q_{xy})|^2=\frac{n_<!}{n_>!}\left(\frac{q_{xy}^2l_H^2}{2}\right)^{n_>-n_<}\times\exp\left(-\frac{q_{xy}^2l_H^2}{2}\right)\left[\mathcal{L}_{n_<}^{(n_>-n_<)}\left(\frac{q_{xy}^2l_H^2}{2}\right)\right]^2. \tag{13}$$

In Eq. (13), $n_<=\min(n,n')$, $n_>=\max(n,n')$, and $\mathcal{L}_m^{(n)}(z)$ is the generalized Laguerre polynomial. By using a generalized Thomas-Fermi screening model, we find

$$V^F_{jj'}(q_{xy}) = \frac{e^2}{2\epsilon_0\epsilon_b q_{xy}} \sum_m \varepsilon^{-1}_{jm}(q_{xy}) \int_{-\infty}^{+\infty} dz \times \int_{-\infty}^{+\infty} dz' \phi^*_m(z)\phi_{j'}(z) \times \exp(-q_{xy}|z-z'|)\phi^*_{j'}(z')\phi_m(z'), \quad (14)$$

where ϵ_b is the average background dielectric constant and $\varepsilon^{-1}_{jm}(q_{xy})$ is the inverse of the static dielectric-function matrix[30]

$$\varepsilon_{ij}(q_{xy}) = \delta_{ij} + \frac{q^{\rm TF}_j}{q_{xy}} \mathcal{F}_{ij}(q_{xy}). \quad (15)$$

In Eq. (15), we have defined the notations

$$\mathcal{F}_{ij}(q_{xy}) = \int_{-\infty}^{+\infty} dz \int_{-\infty}^{+\infty} dz' |\phi_i(z)|^2 \times \exp(-q_{xy}|z-z'|)|\phi_j(z')|^2, \quad (16)$$

and the inverse of the Thomas-Fermi screening length

$$q^{\rm TF}_j = \frac{e^2}{2\pi l^2_H \epsilon_0\epsilon_b} \sum_n \frac{1}{\sqrt{2\pi\Gamma^2_j}} \times \exp\left\{ \frac{-[\mu_c - E_j - (n-\frac{1}{2})\hbar\omega_{cj}]^2}{2\Gamma^2_j} \right\}, \quad (17)$$

where we have assumed a Gaussian form of the Landau-level broadening. The uniform broadening of Landau level superposed on the jth subband in Eq. (17) is taken as[31]

$$\Gamma^2_j = \frac{1}{2\pi}\hbar\omega_{cj}\frac{\hbar}{\tau}, \quad (18)$$

where τ is the relaxation time of electrons by scattering and can be determined from the sample mobility. This is a result of the Born approximation.

In our numerical calculation, we have chosen the well material as GaAs and the barrier material as $Al_xGa_{1-x}As$. The sample parameters are set as $x=0.3$, $T=77$ K, $d_W=140$ Å, $d_B=30$ Å, $V_0=0.83x$, $m_W=0.0665$, $m_B=0.0665+0.0835x$, $n_{2D}=4.2\times10^{11}$ cm^{-2}, $\epsilon_W=12.02$, $\epsilon_B=12.02-2.925x$, and $\tau=2.8\times10^{-11}$ sec.

In Fig. 1 the calculated landau levels E_{nj} are shown as a function of magnetic field B. The labels n and j are for the Landau quantum number and subband index, respectively. The dashed line is for the chemical potential μ_c from which the population and depopulation of each Landau level can be seen. Because the Landau-level broadening is proportional to B, the density of states becomes nonzero far away from the center of Landau level (inside the Landau gap) when $B>9$ T. This makes the chemical potential μ_c deviate downward from E_{11}. Similar reasoning can explain the deviation of chemical potential upward from $E_{1,2}$ when $B\leqslant 9$ T. As $B>9$ T, both the tunneling ($\Delta j=1,\Delta n=0$) and Landau ($\Delta n=1,\Delta j=0$) gaps are found to be almost constant. When $B\leqslant 9$ T, the tunneling gap is greatly reduced and the Landau gap, on the other hand, shows only a slight change in the figure.

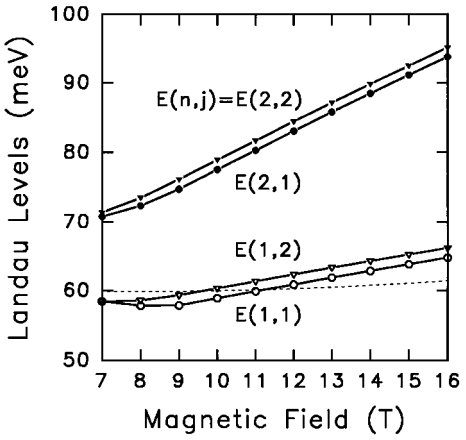

FIG. 1. Landau levels as a function of the magnetic field B. The Landau-level label $E(n,j)$ corresponds to the notation E_{nj} in the text, where n is the Landau label and j is the subband index. The dashed line is for the chemical potential μ_c.

Figure 2 displays the screened exchange energies V^F_{nj} in the same magnetic-field region. The negative exchange energy first increases from high magnetic field down to $B=9$ T, and then starts to decrease for $B\leqslant 9$ T. The reason for this change can be explained as follows. When the magnetic field is reduced down to $B=9$ T, one of the tunneling-split first Landau levels E_{11} becomes gradually populated. As a result, the negative exchange interaction V^F_{nj} increases with the population of Landau level E_{11}, where the screening effects on the exchange interaction play only a negligible role as another tunneling-split first Landau level is depopulated. However, as we further bring down the magnetic field, both tunnel-split first Landau levels E_{11} and E_{12} are filled as shown in Fig. 1. In this case, the screening effects on the exchange interaction becomes dominant. Therefore, the negative exchange energies V^F_{nj} are all reduced. Furthermore, we find that the reduction of the negative exchange energies V^F_{n1} is larger than that of V^F_{n2}, as one can see from Fig. 2.

In Fig. 3 we present the calculated tunneling gap as a function of the magnetic field B by taking $\Delta j=1$ for the first

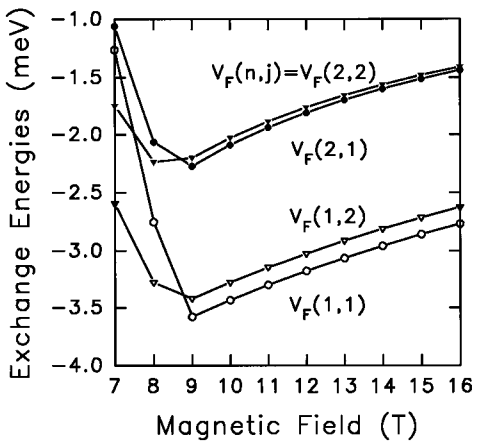

FIG. 2. Exchange energies as a function of the magnetic field B. The exchange-energy label $V_F(n,j)$ corresponds to the notation V^F_{nj} in the text.

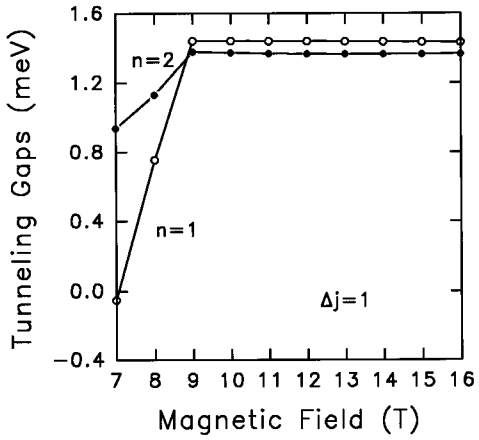

FIG. 3. Tunneling gap $E_{n2}-E_{n1}$ as a function of the magnetic field B for the Landau levels $n=1$ and 2.

$(n=1)$ and second $(n=2)$ Landau levels. We find that the tunneling gaps for both $n=1$ and 2 remain constant for $B>9$ T. Because the magnitude of the tunneling gap is around ~ 1 meV, which is on the same order of or even less than the absolute values of the exchange energies, the strong reduction of the negative exchange energies V_{n1}^F in comparison to that of V_{n2}^F for $B\leqslant 9$ T brings down the tunneling gaps for both $n=1$ and 2. There is an approximately linear B dependence for the tunneling gap in this region. Moreover, the difference in the reduction of exchange energies V_{11}^F and V_{12}^F even exceeds the tunneling gap in the absence of the exchange interaction. As a consequence, the tunneling-split Landau level E_{12} becomes lower than E_{11}, seen as a negative tunneling gap for $n=1$ at $B=7$ T, and then the ground state is switched to E_{12}. This tunneling-split Landau level crossing should be observed in the cyclotron resonance as an anticrossing feature when one reduces the magnetic field below 9 T.

Figure 4 exhibits the Landau gaps as a function of the magnetic field B by taking $\Delta n=1$ for both $j=1$ symmetric and $j=2$ antisymmetric states. Since the Landau gaps ~ 10 meV as shown in Fig. 1 are usually much larger than the exchange energies as shown in Fig. 2, there is no discernible difference between two Landau gaps in the figure when the

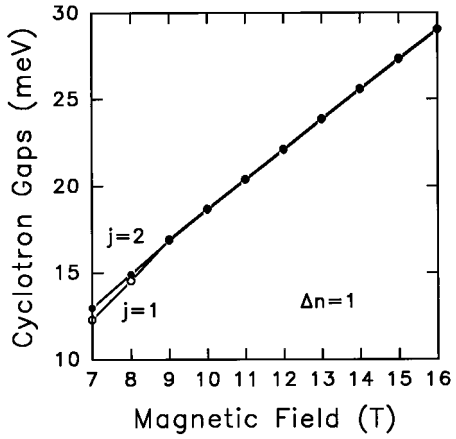

FIG. 4. Landau gap $E_{2j}-E_{1j}$ as a function of the magnetic field B for the subbands $j=1$ and 2.

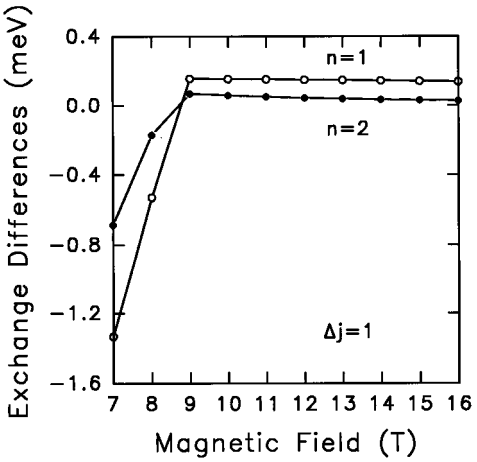

FIG. 5. Difference in the exchange energies $|V_{n1}^F|-|V_{n2}^F|$ as a function of the magnetic field B for the Landau levels $n=1$ and 2.

magnetic field $B>9$ T. When $B\leqslant 9$ T, the Landau gap for $j=1$ is slightly lower compared to that for $j=2$.

In order to support the explanation of the features observed in the tunneling gaps shown in Fig. 3, we plot the differences of the exchange energies $|V_{n1}^F|-|V_{n2}^F|$ as a function of the magnetic field B by taking $\Delta j=1$ for both $n=1$ and 2 as shown in Fig. 5. Clearly, very similar features occur in both Figs. 3 and 5. The negative value of the differences at $B\leqslant 8$ T indicates that the reduction of the exchange energy for $j=1$ is larger than that of $j=2$. However, these differences become approximately independent of B for $B>9$ T.

In Fig. 6 we present the differences of the exchange energies $|V_{1j}^F|-|V_{2j}^F|$ as a function of the magnetic field B by taking $\Delta n=1$ for both $j=1$ and 2. When the magnetic field $B>9$ T, the difference for $j=1$ is slightly larger than that of $j=2$ and their separation remains constant in this region. As B is lowered from $B=9$ T, the reduction of the difference for $j=1$ is faster than that of $j=2$. As a result, the Landau gap for $j=1$ is slightly lower compared to that for $j=2$, as seen in Fig. 4. However, because these two differences are so small compared to the Landau gaps in the absence of the

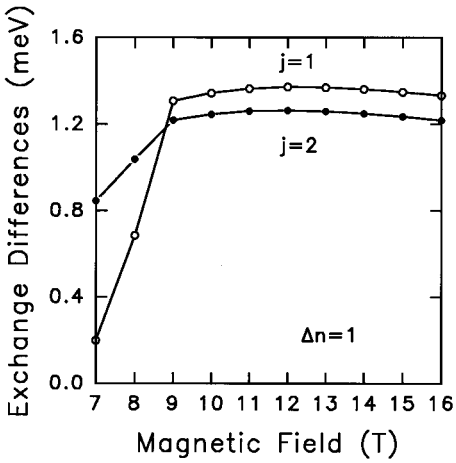

FIG. 6. Plot of the difference in the exchange energies $|V_{1j}^F|-|V_{2j}^F|$ as a function of the magnetic field B for the subbands $j=1$ and 2.

exchange energies, we can observe only very little effects in the Landau gaps, as shown in Fig. 4.

In conclusion, we have performed a self-consistent screened Hartree-Fock calculation by including the Landau quantization of electrons in the presence of the perpendicular magnetic field in a double-quantum-well structure. Therefore, the theory in Ref. 28 has been generalized. Our theory should be applicable to both low ($B<9$ T) and strong magnetic-field ($B>9$ T) cases. The generalized Thomas-Fermi screening model has been used to include the effect of a screened exchange interaction. This has generalized the work of Ref. 27. We have found the features of the approximately linear increase of the tunneling gap at low magnetic fields ($B<9$ T) and the switching of the ground state between two tunneling-split first Landau levels. We have explained these features as a consequence of the increase of screening effects on the exchange interaction as both the tunneling-split first Landau levels are filled. With a thick barrier, the same model can be applied in the Coulomb gap region, where we expect the exchange interaction to play an even more important role in the tunneling gap.

We would like to thank Professor G. Gumbs of Hunter College for his helpful discussions. One of the authors (D.H.) was supported by the National Research Council.

[1] G. S. Boebinger, H. W. Jiang, L. N. Pfeiffer, and K. W. West, Phys. Rev. Lett. **64**, 1793 (1990).
[2] Y. W. Suen, J. Jo, M. B. Santos, L. W. Engel, S. W. Hwang, and M. Shayegan, Phys. Rev. B **44**, 5947 (1991).
[3] K. Ensslin, M. Sundaram, A. Wixforth, J. H. English, and A. C. Gossard, Phys. Rev. B **43**, 9988 (1991).
[4] L. Brey, Phys. Rev. Lett. **65**, 903 (1990).
[5] A. H. MacDonald, P. M. Platzman, and G. S. Boebinger, Phys. Rev. Lett. **65**, 775 (1990).
[6] X. M. Chen and J. J. Quinn, Phys. Rev. Lett. **67**, 895 (1991).
[7] M. Shayegan, J. Jo, Y. W. Suen, M. B. Santos, and V. J. Goldman, Phys. Rev. Lett. **65**, 2916 (1990).
[8] Y. W. Suen, L. W. Engel, M. B. Santos, M. Shayegan, and D. C. Tsui, Phys. Rev. Lett. **68**, 1379 (1992).
[9] J. P. Eisenstein, G. S. Boebinger, L. N. Pfeiffer, K. W. West, and S. He, Phys. Rev. Lett. **68**, 1383 (1992).
[10] S. He, F. C. Zhang, X. C. Xie, and S. Das Sarma, Phys. Rev. B **42**, 11 376 (1990).
[11] V. Halonen, Phys. Rev. B **47**, 10 001 (1993).
[12] S. He, X. C. Xie, S. Das Sarma, and F. C. Zhang, Phys. Rev. B **43**, 9339 (1991).
[13] A. H. MacDonald and S. C. Zhang, Phys. Rev. B **49**, 17 208 (1994).
[14] L. Brey and C. Tejedor, Phys. Rev. B **44**, 10 676 (1991).
[15] H. A. Fertig, Phys. Rev. B **40**, 1087 (1989).
[16] R. Decca, A. Pinczuk, S. Das Sarma, B. S. Dennis, L. N. Pfeiffer, and K. W. West, Phys. Rev. Lett. **72**, 1506 (1994).
[17] S. Das Sarma and P. I. Tamborenea, Phys. Rev. Lett. **73**, 1971 (1994).
[18] J. A. Simmons, S. K. Lyo, N. E. Harff, and J. F. Klem, Phys. Rev. Lett. **73**, 2256 (1994).
[19] G. S. Boebinger, A. Passner, L. N. Pfeiffer, and K. W. West, Phys. Rev. B **43**, 12 673 (1991).
[20] A. P. Heberle, M. Oestreich, S. Haacke, W. W. Rühle, J. C. Maan, and K. Köhler, Phys. Rev. Lett. **72**, 1522 (1994).
[21] A. Kurobe, M. Pepper, and G. A. C. Jones, Phys. Rev. B **50**, 4889 (1994).
[22] G. Rainer, J. Smoliner, E. Gornik, G. Böhm, and G. Weimann, Phys. Rev. B **51**, 17 642 (1995).
[23] S. K. Lyo, Phys. Rev. B **50**, 4965 (1994).
[24] P. Středa, P. Vašek, and M. Cukr, Phys. Rev. B **51**, 11 144 (1995).
[25] J. P. Eisenstein, L. N. Pfeiffer, and K. West, Phys. Rev. Lett. **69**, 3804 (1992).
[26] K. M. Brown, N. Turner, J. T. Nicholls, E. H. Linfield, M. Pepper, D. A. Ritchie, and G. A. C. Jones, Phys. Rev. B **50**, 15 465 (1994).
[27] S.-R. Eric Yang and A. H. MacDonald, Phys. Rev. Lett. **70**, 4110 (1993).
[28] G. Gumbs and G. R. Aĭzin, Phys. Rev. B **51**, 7074 (1995).
[29] A. H. MacDonald, J. Phys. C **18**, 1003 (1985).
[30] K. Esfarjani, H. R. Glyde, and V. Sa-yakanit, Phys. Rev. B **41**, 1042 (1990).
[31] T. Ando, A. B. Fowler, and F. Stern, Rev. Mod. Phys. **54**, 437 (1982).